PHYSICAL REVIEW B VOLUME 11, NUMBER 10 15 MAY 1975

# The electronic contribution to the $c$-axis elastic constants of hexagonal crystals

J. F. Green
*11914 Beltsville Road, Apt. 16, Beltsville, Maryland 20705*

I. L. Spain
*Laboratory for High Pressure Science, Department of Chemical Engineering, University of Maryland, College Park, Maryland 20742*

(Received 13 December 1973)

The effect of $c$-axis elastic strain on the first Brillouin zone for hexagonal crystals is determined. The electronic contribution to $c$-axis elastic moduli is estimated for graphite, a semimetal, and boron nitride, an insulator, using the parabolic and other band models. It is found that a large contribution to the elastic constants can arise from the effect of strain on the electronic energy, arising from a redistribution of electrons within the strained Brillouin zone, or from changes in the bulk electronic properties. It is shown that experimental $c$-axis moduli for graphite can be described empirically if both ion-ion and electron band energies are considered.

## I. INTRODUCTION

In a previous publication,[1] the authors obtained experimental values for the $c$-axis elastic parameters, $C_{33}$ and $C_{44}$, of graphite and their strain derivatives. These measurements allowed a direct comparison to be made with theoretical predictions based on simple pairwise ion-ion models of the interplanar force.[2] A serious discrepancy was demonstrated between the computed ratio, $C_{44}/C_{33}$, and that obtained experimentally, as suggested before by several authors.[3–5] This relative insensitivity of short-range isotropic potentials to $c$-axis shear is a direct consequence of large interplanar spacing compared with in-plane spacing. In-plane structural details, seen from other planes, are unimportant mathematically to an excellent degree of approximation in such models, so that the $c$ planes can be represented as uniform carbon sheets. As a result of this difficulty, the authors were led to an examination of electron band contributions to the interplanar moduli.

The manner in which electrons influence certain crystal elastic moduli is readily illustrated by use of the Brillouin-zone picture. As a Brillouin zone distorts in response to homogeneous crystal strain, electrons are transferred from one region in $k$ space to another. If this redistribution leads to an energy change to second order of strain, an electronic contribution is made to the associated elastic modulus. For an unfilled band, it may be possible for the altered electron assembly to undergo relaxation, effecting further changes in the elastic energy. Another possibility is that the energy levels of the electrons are changed by the applied strain, for example, through changes in interplanar overlap energies. So far, theory has concentrated exclusively on crystals and strains in which the electrons generally respond only by changing the radial displacement from the Brillouin-zone center, permitting use of convenient mathematical approximations.[6–13] The situation is more complex in hexagonal crystals, where the elastic moduli are very sensitive to the details of the energy-band structure. In this paper, the Brillouin zone for the $c$-axis strained crystal is developed in Sec. II, and the electronic contributions to the elastic moduli $C_{33}$ and $C_{44}$ then computed for simplified energy-band models in Sec. III. It is demonstrated that electronic contributions are important for both elastic constants. Other electronic contributions to the $c$-axis moduli are also discussed in Sec. III.

## II. FIRST BRILLOUIN ZONE FOR $c$-AXIS STRAINED HEXAGONAL CRYSTALS

A hexagonal unit cell can be defined by the three translation vectors illustrated in Fig. 1.[14] The Brillouin zone for $c$-axis shear is examined first. Assume a shear such that a material displacement vector transforms, according to the rule

$$(x, y, z) \rightarrow (x, y, z + \delta x) , \tag{1}$$

where $(x, y)$ lie in the $c$ plane and $\delta$ is the shear parameter. The only nonzero strain from (1) is[14]

$$\epsilon_5 = \delta \quad \text{(Voigt notation)} . \tag{2}$$

The $c$-axis elastic energy density $W$ for hexagonal crystals is[14]

$$W = \tfrac{1}{2} C_{44}(\epsilon_4^2 + \epsilon_5^2) + \tfrac{1}{2} C_{33} \epsilon_3^2 . \tag{3}$$

From (2) and (3) one finds

$$\left. \frac{\partial^2 W}{\partial \delta^2} \right|_{\delta=0} = C_{44} . \tag{4}$$

Under the shear strain, (1), unit-cell translation vectors become

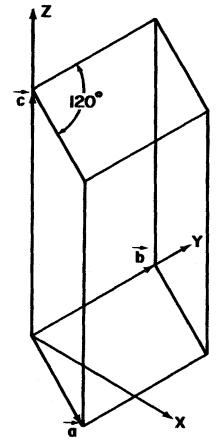


FIG. 1. Unit-cell translation vectors for a hexagonal crystal.

$$\vec{a} = a(\tfrac{1}{2}\sqrt{3},\ -\tfrac{1}{2},\ \delta\tfrac{1}{2}\sqrt{3}),$$
$$\vec{b} = a(0,\ 1,\ 0), \qquad (5)$$
$$\vec{c} = c(0,\ 0,\ 1).$$

Corresponding primitive translation vectors for the reciprocal lattice (see Fig. 2) are

$$\vec{A} = (2\pi/a)(2/\sqrt{3},\ 0,\ 0),$$
$$\vec{B} = (2\pi/a)(1/\sqrt{3},\ 1,\ 0), \qquad (6)$$
$$\vec{C} = (2\pi/c)(-\delta,\ 0,\ 1).$$

In $k$ space, only the $C$ vector is altered. However, since $c$-axis shear causes a break of hexagonal symmetry, the first Brillouin zone becomes complicated (see Figs. 3–5 for representations). In Fig. 5 dashed vectors point to several shear-translated reciprocal-lattice positions in the plane directly above the origin $C$ plane.

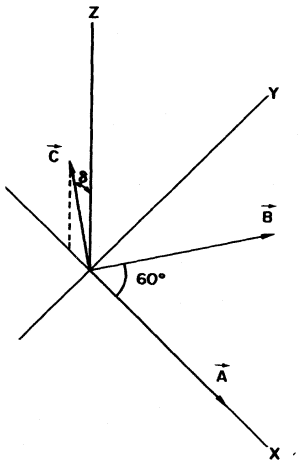


FIG. 2. Reciprocal-lattice vectors for a $c$-axis-sheared hexagonal crystal.

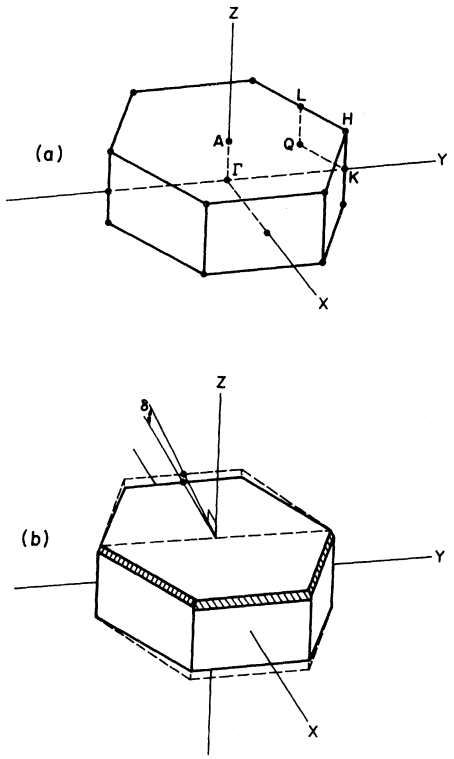


FIG. 3. (a) First Brillouin zone for an unstrained crystal showing symmetry points of interest. (b) First Brillouin zone for a $c$-axis sheared crystal (solid lines). The unstrained zone is shown for comparison (dashed lines).

Referring to Fig. 4, one can interpret the effects of $c$-axis shear on the Brillouin zone. With new axes, $Z'$ parallel to the instantaneous $C$ vector, $X'$ perpendicular to $Z'$, and $Y$ unchanged, the zone has expanded along $C$ by a factor $(1+\delta^2)^{1/2} \approx 1+\frac{1}{2}\delta^2$. $C$-plane width along $X'$ has increased by the same factor, while $C$-plane width along $Y$ is unchanged. These volume gains are counterbalanced by "clipping" of the zone corners.

In sum, the zone is sheared parallel to the ambient $C$ plane, shifting wedge-shaped portions of the unstrained zone further from the origin. A smaller $[O(\delta^2)]$ volume is "clipped" from the outer corners of these wedges and "smeared" along the zone boundaries, half along the boundary $C$ planes and half along the lateral sides. This picture is quite useful for visualizing changes in total zone energy as charge carriers are moved about within the Brillouin zone undergoing strain.

Under compressive strain, the Brillouin zone retains all the symmetry of the unstrained zone, but changes its $Z$ dimension. The electronic compressive $c$-axis modulus, $C_{33}^{f}$, is defined[14]

$$C_{33} = \frac{\partial^2 W}{\partial \epsilon_3^2}\bigg|_{\epsilon_3=0} = c^2 \frac{\partial^2 W}{\partial c^2}\bigg|_{\epsilon_3=0}. \qquad (7)$$

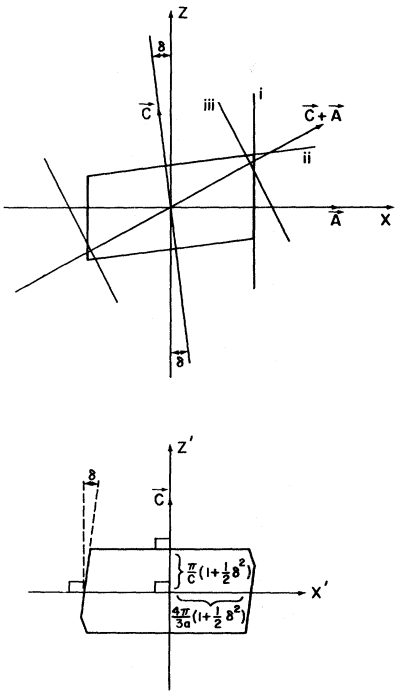


FIG. 4. Cross section of the strained Brillouin zone in the $X$-$Z$ plane. Axes appropriate to the strained zone are designated by primes. Lines (i), (ii), (iii) are defined in Appendix A.

## III. $c$-AXIS ELECTRONIC MODULI

To compute the $c$-axis electronic moduli and their change with $c$-axis compressive strain, it is necessary to choose an explicit electron energy dispersion model. Electron energy density for a filled strained Brillouin zone is then calculated by integration of the dispersion equation over the zone volume. This result can then be introduced into Eqs. (4) and (7) to obtain $C_{44}$ and $C_{33}$. Modifications are made subsequently for deviations from a completely filled zone.

Although some calculations have been made of the electron dispersion relations in graphite and boron nitride within the Brillouin zone (to be discussed in Sec. IV), the results have been limited to high-symmetry directions and are therefore not capable of being applied here. Instead, for computational purposes, the simpler models given by Eqs. (8) have been used. Surprisingly, the calculated electronic moduli were found to be relatively insensitive to change in the dispersion equation.

In this paper, calculations were made for hexagonal crystals using the partial dispersion relations

$$E(k_x, k_y) = \frac{\hbar^2}{2m_1}(k_x^2 + k_y^2), \qquad \text{parabolic in plane}$$

$$= \frac{\hbar^2}{2m_1}\left(\frac{2\pi}{\sqrt{3}a}\right)|k_x^2 + k_y^2|^{1/2}, \qquad \text{linear in plane}$$

$$E(k_z) = \frac{\hbar^2}{2m_3}k_z^2, \qquad \text{parabolic } C \text{ axis}$$

$$= \frac{\hbar^2}{2m_3}\left(\frac{\pi}{c}\right)|k_z^2|^{1/2}, \qquad \text{linear } C \text{ axis} \tag{8}$$

where $\vec{k}$ is the electronic wave vector with origin at $\Gamma$. In these dispension relationships, the sign of the mass parameters is used to define whether the energy increases or decreases as $k$ increases from the zone center. $m_3$ is taken to specify the electronic mass for displacements parallel to the instantaneous $C$ axis, while $m_1$ is for displacements perpendicular to this axis. Filled-zone two-electron $c$-axis elastic moduli are designated formally by the following equations:

$$C_{33} = \frac{2}{(2\pi)^3}\frac{\partial^2}{\partial\epsilon_3^2}\int_{BZ(\epsilon_3)} E(\vec{k})\,d^3k\Big|_{\epsilon_3=0},$$
$$C_{44} = \frac{2}{(2\pi)^3}\frac{\partial^2}{\partial\delta^2}\int_{BZ(\delta)} E(\vec{k})\,d^3k\Big|_{\delta=0}. \tag{9}$$

Note that we have assumed that the dispersion equation is invariant under $c$-axis strains.

Leigh[6] and other[7–10] have used a dispersion equation for cubic lattices which exhibits the influence of the Brillouin-zone boundaries. Calculation using the Leigh relationship has not yet been attempted here owing to the relatively larger importance of zone corner effects ("clipping") for shear in hexagonal lattices. Nonetheless, significant physical aspects of the present model may be examined sufficiently closely without recourse to these more complex dispersion functions.

### A. Theoretical electronic moduli

Theoretical electronic elastic moduli, $C_{33}$ and

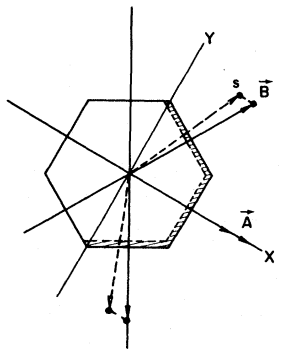


FIG. 5. Cross section of the Brillouin-zone alteration by $c$-axis shear. Solid lines are in the $X$-$Y$ plane, broken lines extend to a plane parallel to the $X$-$Y$ plane but at a $C$-axis spacing $2\pi/c$. Point S is defined in Appendix A. The shaded region defines the clipped region of the zone.

TABLE I. Theoretical electronic elastic parameters for completely filled two-electron band.[a]

| | Elastic parameter | Contribution from in-plane dispersion | Contribution from out-of-plane dispersion |
|---|---|---|---|
| Parabolic dispersion model ($E \sim k^2$) | $C_{33}$ | $2\beta \frac{1}{m_1^*}$ | $\frac{36}{5}\beta\frac{\lambda}{m_3^*}$ |
| | $\frac{\partial C_{33}}{\partial \epsilon_3}$ | $-6\beta \frac{1}{m_1^*}$ | $-36\beta \frac{\lambda}{m_3^*}$ |
| | $C_{44}$ | $\beta(\frac{6}{5}\lambda - 1)\frac{1}{m_1^*}$ | $-\frac{6}{5}\beta \frac{\lambda}{m_3^*}$ |
| | $\frac{\partial C_{44}}{\partial \epsilon_3}$ | $-\beta(\frac{18}{5}\lambda - 1)\frac{1}{m_1^*}$ | $\frac{18}{5}\beta \frac{\lambda}{m_3^*}$ |
| Linear dispersion model ($E \sim \lvert k \rvert$) | $C_{33}$ | $2.53\beta \frac{1}{m_1^*}$ | $10.8\beta \frac{\lambda}{m_3^*}$ |
| | $\frac{\partial C_{33}}{\partial \epsilon_3}$ | $-7.59\beta \frac{1}{m_1^*}$ | $-54\beta \frac{\lambda}{m_3^*}$ |
| | $C_{44}$ | $0.632\beta(1.20\lambda - 1)\frac{1}{m_1^*}$ | $-0.9\beta \frac{\lambda}{m_3^*}$ |
| | $\frac{\partial C_{44}}{\partial \epsilon_3}$ | $-0.632\beta(3.61\lambda - 1)\frac{\lambda}{m_1^*}$ | $2.7\beta \frac{\lambda}{m_3^*}$ |

[a] $\lambda = \left(\frac{\pi}{c}/p\right)^2$; $p = (2\pi/\sqrt{3}a)$; $m^* = m/m_0$; $\beta = \frac{2}{(2\pi)^3}\frac{\hbar^2}{m_0}\frac{10\sqrt{3}}{9}\rho^4\left(\frac{\pi}{c}\right)$.

$C_{44}$, and their $c$-axis compressive strain derivatives were computed by introducing the dispersion relationships (8) into the definitions (9). Results are presented parametrically in Table I. Several combinations of the model can be formed readily. For example, suppose

$$E(\vec{k}) = \frac{\hbar^2}{2m_1}(k_x^2 + k_y^2) + \frac{\hbar^2}{2m_3}\left(\frac{\pi}{c}\right)(k_z^2)^{1/2} .$$

From Table I one finds

$$C_{33} = 2\beta(1/m_1^*) + \tfrac{27}{5}\beta(\lambda/m_3^*) .$$

In Sec. III B, theoretical moduli are examined for graphite and boron nitride. (Details of the present calculations can be obtained on request.)

### B. Electronic moduli for graphite, boron nitride

Lattice constants for the hexagonal isoelectronic series, graphite (C), boron nitride (BN), and beryllium oxide (BeO), are compiled in Table II.[15] Included are the derived parameters, $\lambda$ and $\beta$, for each material. The values for boron nitride and graphite are quite similar, although atomic positions within the unit cell are different. Beryllium oxide is a strongly ionic structure with markedly smaller $c/a$ ratio than boron nitride or graphite. No theoretical or experimental moduli are known to the authors, in the literature, so that this compound will not be discussed further.

Previous investigations of the interplanar binding in graphite have centered upon models using ion-ion interactions only.[2,5,16–18] The calculated elastic ratio, $C_{44}/C_{33}$, from these interactions is an order of magnitude too small, in view of experiment. Similar calculation for boron nitride, but using an ion-ion potential which includes an ionic (ion-charge) term, gives a $C_{44}/C_{33}$ ratio close to that measured in graphite.[19] Although no shear measurements have been made on boron nitride, overall mechanical characteristics of this substance are very similar to graphite. It is reasonable, then, to assume that the actual elastic ratio in boron nitride and graphite are approximately equal. Consequently, one can speculate that while a purely ion-ion model suffices for boron nitride, it fails badly for graphite.

*Case* 1. In contrast with these earlier ion-ion models, let us assume here that the interplanar forces in boron nitride and graphite are entirely electronic in nature, the ion-ion forces being negligible.

TABLE II. Hexagonal lattice parameters for C, BN, and BeO.

| | C | BN | BeO |
|---|---|---|---|
| $a$ (Å) | 2.46 | 2.50 | 2.70 |
| $c$ (Å) | 6.71 | 6.66 | 4.38 |
| $\lambda$ ($10^{-1}$) | 1.01 | 1.06 | 2.76 |
| $\beta$ ($10^{10}$ N/m$^2$) | 4.22 | 4.14 | 4.45 |

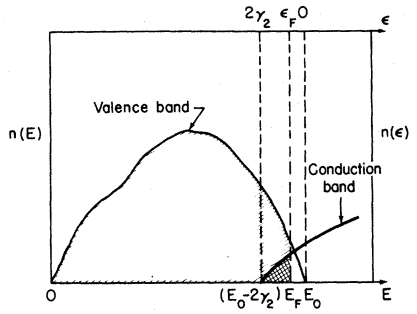


FIG. 6. Energy dispersion relationship for principal symmetry directions from Doni and Parravicini (Ref. 21). Only the highest valence and lowest conduction bands are shown, in both cases derived from atomic $p_z$ orbitals. (a) Boron nitride ($\epsilon_g \sim 5$ eV). (b) graphite (bands overlap by $\sim 0.04$ eV).

First, one must choose electron dispersion equations appropriate to boron nitride and to graphite. Typical results of electron band theory for these materials are shown in Fig. 6 [see also Fig. 3(a)]. Since $c$-axis strains affect only electrons close to the first Brillouin-zone boundary, only that portion of the band structure is of interest here. Unfortunately, energy changes are not known along the $ALH$ (boundary $C$) planes. This region is clearly of great importance to the electronic moduli. The two lower bands have opposite behavior in the $QL$ direction on the $QLKH$ (lateral side) planes—one gaining, the other losing energy. Rather than attempt to deduce actual band details in the neighborhood of the Brillouin-zone boundary, we have calculated the electronic elastic parameters using both linear and parabolic energy bands, wherein these models are understood to apply only near the Brillouin-zone boundary and not necessarily to the remainder of the zone.

Second, if the interplanar binding is due entirely to electronic effects, the interplanar electronic energy density $W$ must be a minimum for $c$-axis strains. This is automatically true for shear. The compressive minimum condition, $\partial W/\partial \epsilon_3 = 0$, yields the constraint

$$\begin{aligned} 1/m_1 &= -\tfrac{9}{5}\,(\lambda/m_3)\,, \quad \text{parabolic band} \\ 1/m_1 &= -2.14\,(\lambda/m_3)\,, \quad \text{linear band}\,. \end{aligned} \tag{10}$$

Equations (10) are understood easily. If $m_1$ and $m_3$ have the same sign, Brillouin-zone energy could be decreased simply by expanding or contracting the zone along the $C$ axis, depending on sign. There must be forces opposite in sign arising from the $m_1$-controlled and the $m_3$-controlled energy dispersion equations.

Introducing Eqs. (10) and values for Table II into Table I, one finds the elastic parameters shown in Table III for case 1. Evidently, the parabolic model can fit experiment somewhat better than the linear model. After adjusting the parabolic mass $m_3$ to fit $C_{33}$ to experiment, one has $m_3 \approx 0.9 m_0$, $m_1 \approx -4.8 m_0$ in the parabolic model. The physical significance of these masses is discussed following case 2.

*Case* 2. In case 1 it was assumed that all $c$-axis binding arose through electronic effects. However, as noted above, other models which employ Lennard-Jones or Buckingham-type potentials to describe a pairwise interplanar ion-ion interac-

TABLE III. Four-electron[a] filled-band theoretical and experimental elastic parameters.

| | $C_{33}$ ($10^{10}$ N/m$^2$) | $C_{44}/C_{33}$ | $\frac{1}{C_{33}}\frac{\partial C_{44}}{\partial \epsilon_3}$ | $\frac{1}{C_{44}}\frac{\partial C_{44}}{\partial \epsilon_3}$ |
|---|---|---|---|---|
| Experiment (a) Graphite[b] | $3.6 \pm 0.1$ | $0.12 \pm 0.01$ | $-14.8 \pm 0.8$ | $-6.0 \pm 2.0$ |
| Theory (case 1) (i) Electronic binding | | | | |
| (a) Parabolic band | $3.07\frac{1}{m_3^*}$ | 0.11 | −7.0 | −6.4 |
| (b) Linear band | $4.73\frac{1}{m_3^*}$ | 0.054 | −7.0 | −6.3 |
| Theory (ii) Ion binding[c] | 3.2 | 0.006 | −15.2 | −12.2 |
| Theory (case 2) (iii) Electronic plus ion binding parabolic band | 3.6 | 0.11 | −15.2 | 0.6 |

[a]Four electrons per state are included to account for the spin and spatial degeneracy.
[b]See Ref. 1 for a recent summary.
[c]See Ref. 2.

tion in graphite and boron nitride have been successful in predicting $C_{33}$ and $(1/C_{33})(\partial C_{33}/\partial \epsilon_3)$. We are thus led to consider as case 2 a model in which the $c$-axis energy is a linear sum of ion-ion energy plus electron band energy. In this model, virtually all the energy resides in the ion-ion contribution, the electron contribution being important only for shearing modes.

Results from one ion-ion calculation, made elsewhere by the authors,[2] using a van der Waals attraction and an exponential core repulsion are shown in Table III under the heading "Ion binding." Since conditions (10) are not valid for case 2, values for $m_1$ and $m_3$ (parabolic) were chosen in Table II such that the experimental moduli, $C_{33}$ and $C_{44}$, are comprised of a linear sum of the respective ion-ion modulus and electronic modulus. Strain derivatives are calculated using the compound moduli, and all theoretical parameters are given in Table III under the heading "Electronic plus ion binding." To fit experiment in case 2, the electron masses (parabolic) are set: $m_3 \approx 3.4 m_0$ and $m_1 \approx -11.1 m_0$.

Clearly, the experimental graphite $c$-axis elastic moduli and their compressive strain derivatives (see Table III) can be fitted reasonably well by a model in which the interplanar binding consists of a mixture of electronic and ion-ion interactions. Only a minor admixture of ion-ion binding is necessary to bring the theoretical electronic moduli, in case 1, into acceptable experimental ranges. Empirical values for the electron masses, based on this supposition, should be

$$m_3 \approx m_0 \; ; \quad m_1 \approx -6 m_0 \; . \tag{11}$$

The condition (11) can be understood in a simple way. The actual dependence of energy on $\vec{k}$ near the Brillouin-zone boundaries must be more complicated than represented in the present model. In essence, the removal of electrons from the clips across the hexagonal faces dominates the energy change, and results in a positive change only if $m_1$ is negative. The energy change resulting from redistribution of electrons in the wedge volumes is relatively smaller.

*Case* 3. The deduced electron masses for cases 1 and 2 are not necessarily representative of the general band structure. Specifically, if one sets $m_1 = m_3 = 2m_0$, characteristic of the general dispersion in graphite, then the electronic elastic moduli are, according to Table I,

$$C_{33} = 11.5 \times 10^{10} \text{ N/m}^2 \; ; \quad C_{44} = -4.22 \times 10^{10} \text{ N/m}^2 \; .$$

Both these moduli are much larger in magnitude than actually observed. The negative $C_{44}$ derives from use of positive mass in the dispersion relationships (8). Under $c$-axis shear, prismatic slices of electrons are removed from the outer edges of the Brillouin zone [see Fig. 3(b)] and "smeared" out in equal amounts along the $C$-plane boundaries and lateral sides. This redistribution decreases the average sizes of $(k_x^2 + k_y^2)$ and $k_z^2$ for the transported electrons. A gain in magnitude of $k_z^2$ for some electrons is obtained through the removal of wedge-shaped regions from along one half of each lateral side of the Brillouin zone and replacement on the adjoining half (see Fig. 4). This latter increase does not offset completely the average loss in $(k_x^2 + k_y^2)$ from the "smearing." Consequently, there is an over-all loss in zone energy, signified by a negative shear modulus (instability under shear). Thus, near the Brillouin-zone boundary, the actual electron dispersion function must deviate substantially from that of the general band, unless other large positive electronic contributions to $C_{44}$ are important.

Further interpretation of these results from simple band models is discussed in Sec. IV.

If it is possible to compute the zone-boundary electron masses for boron nitride through scaling of general band calculations with those for graphite, then a complete set of predictions can be made also for the boron nitride $c$-axis elastic moduli. As seen in Fig. 6, band energies in boron nitride are smaller than in graphite by a factor approximately equal to 4. One might reasonably expect that, for boron nitride, electronic moduli are correspondingly smaller than for graphite. Such moduli would surely be too small to be of major interest. Because it is unlikely that an appreciable ionic bond character can be associated with the graphite lattice, one could propose that interplanar interactions which control $c$-axis shear movement in graphite are primarily electron-band-related, while those in boron nitride are mainly ion-charge–ion-charge-related.

### C. Effect of overlap electrons

Graphite in reality is a semimetal rather than an insulator, as in the model above. Consideration must be taken of the small electron overlap, from one of the valence bands, along the first Brillouin-zone lateral edges.

The lateral sides of the first Brillouin zone do not change perpendicular displacement from the origin for either of the $c$-axis strains, $\epsilon_3$, $\epsilon_5$. As a result, it is relatively easy to compute the overlap corrections to the closed-band electronic moduli. Under $c$-axis compressive strain, all Brillouin-zone symmetry is preserved while only the $c/a$ ratio changes; under $c$-axis shear strain, only a small fraction of the hole volume is affected, while overlap electrons are completely unshifted. Normally, it is assumed that the electron "bubble" is fixed to the associated strain-displaced Brillouin-zone surface, allowing for relaxation through

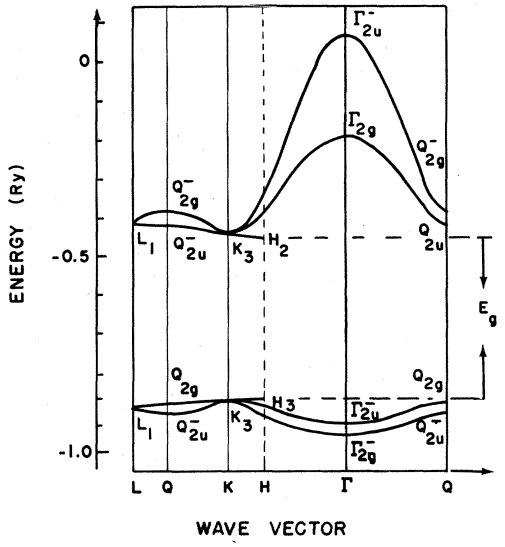


FIG. 7. Sketch of the density of states for the semimetal graphite. The valence band, of width $E_0$, overlaps the conduction band by $2\gamma_2$, where $\gamma_2$ is a next-nearest layer overlap integral.

exchanges with the other "bubbles" in the zone. Evidently in graphite, during $c$-axis shear strain, the relaxed overlap electron assembly is indistinguishable from the unstrained assembly, thereby not contributing to the shear strain energy.

The additive modification to the energy density, $W$, from electron overlap may be obtained from the total electronic energy in the band at $T=0\,^\circ$K:

$$W=\int_0^{E_F} En(E)\,dE\,, \tag{12}$$

where $n(E)$ is the electronic density of states.

The energy density $W$ is here measured relative to the bottom of the valence band of width $E_0$ (see Fig. 7). Equation (12) may be rewritten as

$$W=\int_0^{E_0} En_v(E)\,dE+\int_{E_0-2\gamma_2}^{E_F} En_c(E)\,dE - \int_{E_F}^{0} En_v(E)\,dE \tag{13a}$$

$$= W_{fb}+\bar{W}(e)-\bar{W}(h)\,, \tag{13b}$$

where $n_v(E)$ and $n_c(E)$ are the densities of states in the valence and conduction bands, respectively; $W_{fb}$, $\bar{W}(e)$, $\bar{W}(h)$ are the energy contributions from the filled valence band, conduction-band electrons, and valence-band holes, respectively. In this expression the valence and conduction bands overlap in the interval $E_0-2\gamma_2$ to $E_0$ (see Fig. 7) where $E_0$ is the valence-band width.

The terms $W(e)$ and $W(h)$ may be written as

$$W(e)=\int_{2\gamma_2}^{E_F}(E_0+\epsilon)n_0(\epsilon)\,d\epsilon=\int_{2\gamma_2}^{E_F}\epsilon n_c(\epsilon)\,d\epsilon+NE_0\,, \tag{14a}$$

$$W(h)=\int_{\epsilon_f}^{0}(E_0+\epsilon)\,n_v(\epsilon)\,d\epsilon=\int_{\epsilon_f}^{0}\epsilon n_v(\epsilon)\,d\epsilon+PE_0\,, \tag{14b}$$

where $\epsilon$ measures electron energies relative to the top of the valence band (Fig. 7), allowing (14a) and (14b) to be evaluated using the dispersion relationship for electrons near the overlap region developed by Slonczewski and Weiss.[20] It may be shown that the first terms in the right-hand side of (14a) and (14b) are negligible (their contribution to $C_{33}$ amounts to $\sim 10^6$–$10^7$ Nm$^{-2}$) and they will be neglected in the following treatment. Thus

$$W\sim W_{fb}+(N-P)E_0 \tag{15}$$

and, since $N=P$ in an intrinsic crystal,

$$W\sim W_{fb}\,. \tag{16}$$

Modification of the $c$-axis shear modulus, $C_{44}$, by electron overlap must be very small, since only a minute fraction of the hole volume in the first Brillouin zone is affected by shear. An approximation can be made of the magnitude of this effect by estimating the ratio of the sheared hole area to the sheared Brillouin-zone area. The hole cross-sectional area $A_h$ at the Brillouin-zone $C$-plane boundary divided by the total $C$-plane boundary area, $A_{ec}$, is approximately

$$A_h/A_{ec}\cong 10^{-5}\,,$$

which is far too small to be important.

### D. Contributions to elastic moduli arising from changes in bulk electronic properties

In all crystals the energy levels are modified to various extent by strains. In a layer material such

as graphite, the dependence of the energy levels on strain can conveniently be described using the tight-binding approximation. Clearly, for $c$-axis strain, only the interplanar distances are changed appreciably, so that only interlayer overlap integrals need be considered. (The $c$-axis linear compressibility is approximately 20 times that in the basal plane.) In this theory, the energy variation with basal wave vector throughout most of the Brillouin zone is controlled by the in-plane (covalent) electronic overlap. This can therefore be taken as approximately invariant under $c$-axis strains. On the other hand, interplanar overlap integrals control the energy variation with out-of-plane wave-vector ($k_z$).

The total electronic energy in the valence and conduction bands, $W$, is given by Eq. (13a). Thus, from Eqs. (9), the $c$-axis elastic compressive constant may be written as

$$C_{33} = \frac{\partial^2}{\partial \epsilon_3^2}\left( t\,\frac{\gamma}{a^2 c}\right) , \tag{17}$$

where $\gamma$ is an average energy difference between the mid-plane [$\Gamma QK$ in Fig. 3(a)] and the $C$-plane [$ALH$ in Fig. 3(a)] boundaries of the Brillouin zone. This energy $\gamma$ is essentially the difference in bandwidth energy ($E_0$) between the three-dimensional and two-dimensional crystal and is proportional to the interplanar overlap energy. The value of $t$, a dimensionless geometric parameter, depends on the energy dispersion relationship in the $C$-axis direction. It is calculated directly from Eq. (12). For reasonable choices of this relationship, $t$ lies in the range 10–15. Differentiating, one finds

$$C_{33}^{\text{bulk}} \sim \frac{t\gamma}{a^2 c}\left(1 + \frac{\partial \ln \gamma}{\partial \epsilon_3} + \frac{1}{\gamma}\,\frac{\partial^2 \gamma}{\partial \epsilon_3^2}\right) \tag{18}$$

Taking a typical value for $\gamma$ ($\sim 0.1$ eV),[21–23] and assuming that $\partial \ln \gamma / \partial \epsilon_3 \sim \partial \ln \gamma_1 / \partial \epsilon_3$, where $\gamma_1$ is the nearest-neighbor interlayer interaction parameter appearing in the band theory of Slonczewski and Weiss,[20] one obtains using experimental data[24–27]

$$C_{33}^{\text{bulk}} \sim 3 \times 10^{10}\ \text{Nm}^{-2} .$$

(In the Slonczewski-Weiss theory, the energy difference between point $K$ and point $H$ is approximately $2\gamma_1$. Thus, the assumed equality of the strain derivatives of $\gamma$ and $\gamma_1$ should be reasonable.) This bulk electronic effect presumably controls a substantial proportion of the $c$-axis compressibility of graphite. Usually, van der Waals forces have been employed to describe this $c$-axis compressibility. While such other theories are mathematically satisfactory, the interplanar interaction in graphite may originate largely in the bulk electronic effect.

An attempt has been made by Santos and Villagra[28] to identify the compressive energy with an ion-electron interaction. Their approach gave a reasonable value for the compressive modulus $C_{33}$. Further calculation by one of us (JFG) shows that the strain derivative is also predicted reasonably by their model. However, their model used a charge distribution which was uniformly smeared across carbon planes, so that no predictions could be made regarding the shear modulus $C_{44}$ or its strain derivative.

In the present case we may also assume that an electronic contribution to the $c$-axis moduli arises from the effect of shear strain on the $c$-axis overlap integrals. By analogy with the above comparison for the compressive modulus $C_{33}$, we may conjecture that a contribution to $C_{44}$, normally described by the Lennard-Jones interatomic potential, arises from this shear dependence of the overlap energy $\gamma$. In principle, this contribution to $C_{44}$ may be calculated from Eqs. (9). However, as pointed out above, hexagonal symmetry is broken by $c$-axis shear. Consequently, simplifying assumptions, which allow the hexagonal crystal interaction matrix to be reduced to a $4\times4$ matrix,[20] no longer hold. Since, in addition, no experimental estimates of the shear dependence of the interlayer overlap integrals exist, no further attempt can be made here to calculate the bulk electronic contributions to $C_{44}$. Since the effect should be at least comparable in magnitude to ion-ion contributions, a calculation is clearly of major interest.

## IV. DISCUSSION OF RESULTS

In Sec. III, the electronic $c$-axis moduli $C_{33}$, $C_{44}$ were calculated for parabolic and linear electron models. It was found that large contributions could be expected from the electronic effect, and that the presence of free carriers in the semimetal graphite would not affect this result appreciably. The dispersion relationships used here were chosen for computational convenience. They allowed the electronic contributions arising from $c$-axis strains of the Brillouin zone to be computed by adjusting, at most, two parameters. It was then shown that good agreement could be obtained with experiment for graphite, if both electronic and ion-ion effects were considered together. The effective mass values obtained were quite different from the general band masses, particularly the effective basal mass, $m_1 \approx -6m_0$. This is discussed below.

First, it must be recognized that the electronic contribution arises from the redistribution of electrons near the *surfaces* of the Brillouin zone, as detailed in Sec. III B. Particular dispersion relationships used here are simply convenient ways of representing differences in electronic energy of these surface electrons. As discussed earlier, if general band electronic effective masses ($m_1 = m_3 \sim 2m_0$) are used to estimate these surface ef-

fects, then an unreasonably large contribution to $C_{33}$ is obtained. This strongly suggests that the bands behave in a more complicated way across the Brillouin-zone $C$-plane boundaries [$ALH$ in Fig. 3(a)] (where the electrons are being diffracted) than across the median planes [$\Gamma KQ$ in Fig. 3(a)], where band calculations[21-23] have been made.

Furthermore, a large negative contribution to $C_{44}$ is obtained if these general band effective mass values are used. This arises primarily from the over-all average decrease in electron wave vector occasioned by the removal of electrons from the clipped regions of the Brillouin zone to the zone $C$-plane boundaries [$ALH$ in Fig. 3(a)]. This result also suggests that the actual dispersion relationship for these surface electrons is more complicated than that proposed. A detailed calculation of the electron energies in the regions near the surface of the Brillouin zone should resolve this uncertainty.

No other satisfactory explanation for the observed ratio, $C_{44}/C_{33}$, in graphite has been proposed, to the knowledge of the present authors. Kelly[29] has suggested that conventional ion-ion potentials could possibly explain the discrepancy in $C_{44}$ for graphite, if a potential with a sharper minimum were used, perhaps corresponding to a pileup of electronic $p_z$ orbitals between atoms in adjacent layers. Such a charge distribution would lead to large energy increases, yielding serious problems with the calculated value for $C_{33}$. Equivalent difficulties are associated with other models which assign fractional electronic charges to interstitial positions between neighboring atoms in the basal plane.

In the absence of other explanations, we have given values for the electronic parameters $m_1$ and $m_3$ in our model to account for the observed $c$-axis moduli and their strain derivatives. It is cautioned that these masses must be interpreted with some care. Detailed calculations using a more realistic disperion relationship are clearly required, but at present no such relationship is available, except near the zone corners.[20]

A detailed theory for the moduli $C_{33}$ and $C_{44}$ should take into account both the effect of transfer of near-surface electrons across the Brillouin zone and the effect of strain on the bulk electronic properties. These bulk and zone-surface effects can certainly give a contribution of the correct order of magnitude to $C_{44}$ while maintaining the correct value for the ratio $C_{44}/C_{33}$. The results obtained here are probably applicable not only to graphite and boron nitride, but also to a wide range of materials having planar structures in which the interlayer forces are weak, and have been described previously by van der Waals dispersion forces.

## ACKNOWLEDGMENTS

The authors wish to thank B. T. Kelly for valuable suggestions. A grant from the United States Atomic Energy Commission is gratefully acknowledged.

[1] J. F. Green, P. Bolsaitis, and I. L. Spain, J. Phys. Chem. Solids 34, 1927 (1973).
[2] J. F. Green and I. L. Spain, J. Phys. Chem. Solids 34, 2177 (1973).
[3] K. J. Komatsu, J. Phys. Solids Jpn. 10, 346 (1955).
[4] G. Dolling and B. N. Brockhouse, Phys. Rev. 128, 1120 (1962).
[5] B. T. Kelly and M. J. Duff, Carbon 8, 77 (1970).
[6] R. S. Leigh, Phil. Mag. 42, 139 (1951).
[7] H. J. Jones, Phil. Mag. 43, 105 (1951).
[8] J. M. Ziman, Adv. Phys. 10, 1 (1961).
[9] J. G. Collins, Phys. Rev. 155, 663 (1967).
[10] R. Chiarodo, J. Green, I. L. Spain, and P. Bolsaitis, J. Phys. Chem. Solids 33, 1905 (1972).
[11] R. W. Keyes, Solid State Phys. 11, 149 (1960).
[12] R. W. Keyes, Solid State Phys. 20, 37 (1967).
[13] A. K. Sreedhar and S. C. Gupta, Phys. Rev. B 5, 3160 (1972).
[14] J. F. Nye, *Physical Properties of Crystals* (Oxford U.P., Oxford, England, 1967).
[15] R. W. G. Wyckoff, *Crystal Structures*, 2nd. ed. (Wiley, New York, 1963).
[16] D. J. Crowell, J. Chem. Phys. 29, 446 (1958).
[17] V. M. Agranovich and L. P. Semenov, J. Nucl. Energy AIB 18, 141 (1961).
[18] L. A. Girifalco and R. A. Lad, J. Chem. Phys. 25, 693 (1956).
[19] J. F. Green, T. K. Bolland, and J. W. Bolland (unpublished).
[20] J. C. Slonczewski and P. R. Weiss, Phys. Rev. 109, 272 (1958).
[21] E. Doni and G. P. Parravicini, Nuovo Cimento B 64, 117 (1969).
[22] C. S. Painter and D. E. Ellis, Phys. Rev. B 1, 4747 (1970).
[23] J. Zupan, Phys. Rev. B 6, 2477 (1972).
[24] R. G. Arkhipov, V. V. Kechin, A. I. Likhter, and Yu A. Pospelov, Zh. Eksp. Teor. Fiz. 44, 1964 (1963) [Sov. Phys.-JETP 17, 1321 (1963)].
[25] J. R. Anderson, W. J. O'Sullivan, and J. E. Schirber, Phys. Rev. 3, 1038 (1967).
[26] E. S. Itskevitch and L. M. Fisher, Zh. Eksp. Teor. Fiz. Pis'ma Red. 5, 141 (1967) [Sov. Phys.-JETP Lett. 5, 114 (1967)].
[27] V. V. Kechin, A. I. Likhter, and G. N. Stepanov, Fiz. Tverd. Tela 10, 1242 (1968) [Sov. Phys. – Solid State 10, 987 (1968)].
[28] E. Santos and A. Villagra, Phys. Rev. B 6, 3134 (1972).
[29] B. T. Kelly (private communication).